Journal of Theoretical and Applied Information Technology
15th February 2018. Vol.96. No 3

ISSN: 1992-8645 www.jatit.org E-ISSN: 1817-3195

HVS BASED NEAR REVERSIBLE DATA HIDING SCHEME USING DCT

[1]T. BHASKAR, [2]D. VASUMATHI

[1]Research Scholar, Department Of Computer Science & Engineering
JNTUH College Of Engineering Hyderabad (Autonomous)
Hyderabad, Telangana, India.
[1]bhalu7cs@gmail.com.

[2]Professor, Department Of Computer Science & Engineering
JNTUH College Of Engineering Hyderabad (Autonomous)
Hyderabad, Telangana, India.

ABSTRACT

In this research, a certain level of modifications to the original content can be acceptable. These schemes are called near-reversible. In this embedded content is allowed to be manipulated and the content can be restored almost to the original content. It has emerged application in remote sensing. In remote sensing application the image is captured while monitoring the damaged regions in the natural disasters such as tsunami, volcanic eruption, etc. proposed scheme have less pixel alterations or coefficients as an alternate to more alterations. In reversible data embedding shows the evidence of low embedding capacity and complexity. Already exist a few near reversible hiding schemes, deals with capacity, robustness and visual quality metrics. when the data is hidden in the image which is unclear, for accessing that image best quality metrics we need to use, generally the conventional mertric PSNR is not sufficient. Therefore, we present an HVS based metrics like PSNR_HVS, PSNR_HVS_M, MSSIM. Using frequency domain transform that evaluates the overall image quality. Hence, the new knowledge on this research paper is design of near-reversible scheme which has wider applications in remote sensing.

Keywords: *HVS (Human Visuval System), Frequency Domain Transform, PSNR_HVS, PSNR_HVS_M And MSSIM*

1. INTRODUCTION

The creation of high capacity digital recording devices and the fast growth in using the Internet technology, though it is a sign of technological growth, is becomes a warning to the multimedia content owners. Since, this improvement made the users to share and distribute the multimedia contents like image, audio, video, etc. easily and illegally. The hidden data [9] can be secret information to cover content for any scheme is designed. Some schemes exact reversibility is cannot be concentrated, because certain more modifications in cover content are allowed those schemes are near reversible schemes. There is a urgent need of near reversible schemes for applications like copyright protection of remote sensing images [6]. A basic task in many image and video processing tools is the visual evaluation, based on objective of digital data. The objective evaluation is done with help of assessment models like Peak Signal-to-Noise Ratio (PSNR) is does not correlate well with viewer's opinion , P_HVS is a metric which calculate Peak signal to noise ratio (PSNR) considering Human Visual System, P_HVS_M [7] is a metric which calculates the between-coefficients contrast masking of DCT basis function, MSSIM index evaluates the overall image quality, contrast sensitivity function [13,14,15] (CSF) measures the ability to see details at low contrast levels and Structural Similarity[8,18,19] (SSIM) index metric checks the similarity between two images where one image should be of perfect quality. These metrics based on Human Visual System[16,17] (HVS) are

ISSN: 1992-8645 www.jatit.org E-ISSN: 1817-3195

developed. The extended research area has been evolving to address the limitations such as many alterations to the pixels or coefficients, low hiding capacity and complexity that exhibit while reversible data hiding. Limiting the triangular trade-off that exists between capacity, robustness and visual quality is challenging. However, for achieving better visual quality, there is a need for HVS based near reversible data hiding schemes. Hence, the research questions that the paper is addressing is the near reversibility of the data embedding scheme. This near reversibility has significant application in remote sensing further is also addresses the use of proper HVS based metrics to access the visual quality.

2. LITERATURE SURVEY AND EXISTING SCHEMES

Barni et al. [5] have introduced the near-lossless paradigm for the first time. They showed that, by forcing a maximum absolute difference between the original and watermarked scene, the near-lossless paradigm makes it possible to decrease the effect of watermarking on remote sensing applications to be carried out on the images.

Ahmed and Moskowitz [10] proposed a semi-reversible frequency domain digital watermarking technique that can be used to authenticate medical images in a distributed diagnosis and home health care environment. There approach is for protecting medical informatics is digital watermarking.

Tang and Huang [11] In this paper, a near-reversible data embedding scheme is proposed based on projection histogram manipulations. Because the projection histograms are relatively stable under common image operations, the attacked image can be restored to a level which is very close to the original image.

Zhang et al. [12] have proposed a near reversible watermarking algorithm based on LSB replacement. Simulation results prove that the watermarked image not only can well hide the watermark information by storing the secondary LSB data of host image and the watermark data in the same bit, but also can be recovered to the original host image to a high extent.

M Fujiyoshi and Hitoshi Kiya[21] the proposed method is based on unification of HS- and LSB substitution-based DH. In the method, lossless compression of the marked image achieve less efficiency and is not flexible in capacity and distortion.

In Existing Scheme, the embedding process uses *Log* function. This scheme partially achieves embedding capacity, robustness and visual quality, but many blocking artifacts can be observed in the embedded image. Thus, this scheme achieves good capacity and reversibility, but it lacks good visual quality which has to be addressed [1,2,3,4].

3. PROPOSED SCHEME

In proposed scheme, the embedding process concentrates on achieving the better visual quality and removing the blocking artifacts. We propose a mathematical function to achieve the above objective. The objective of the proposed solution is to improve the visual quality of the images i.e. avoiding the blocking artifacts. In existing system, reference image taken as input is portioned into 8×8 blocks of intensity values and 2- dimensional DCT is applied on each block. Then each block is divided by quantization table of 8×8 block. In embedding process, the data is embedded in all non-zero DCT coefficients i.e. the block whose number of non-zero DCT coefficients is greater than zero then the data is embedded in that block is embedded as shown in figure 3.1. The mathematical function is used for embedding data. After this process the difference obtained between the original Non-zero AC coefficient[20] and data embedded coefficient is much greater as a result the watermarked image obtained has blocking artifacts.

The extraction process extracts the image with well suitable equation and the HVS metrics used such as PSNR, PSNR_HVS, PSNR_HVS_M, MSSIM and reversibility schemes give good values with good visual quality.

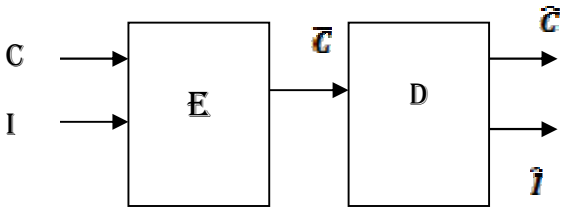

Figure 3.1: Generic Data Embedding And Extraction Procedure

Journal of Theoretical and Applied Information Technology
15th February 2018. Vol.96. No 3

ISSN: 1992-8645 www.jatit.org E-ISSN: 1817-3195

The data embedding procedure is given by $E(C,I) = \bar{C}$ and *the data* extraction procedure is given by $D(C) = (\hat{C},\hat{I})$. *Here* $\hat{I}$ *is the* extracted data and $\hat{C}$ is the cover object after extracting the data. When $C = \hat{C}$ and $I = \hat{I}$, we define the data extraction procedure as reversible, otherwise it is irreversible.

3.1 Data Embedding Procedure

The data is embedded in all non-zero AC Coefficients pixels in each block except the blocks where all AC Coefficients are equal to zero. For better visual quality, the design is proposed to reduce the modifications to the original coefficients i.e. the watermarked coefficients are retained to nearer value of original coefficients.

Algorithm:

1. Take an input image *I* and
2. Partition I using DCT I$\rightarrow \{B_1,B_2,\ldots.B_l\}$
   For each$B_j \in I$, where $1 \le j \le 8$
   (a) Quantize the DCT coefficients in $B_j$as below.

for $i_1 \leftarrow 1$ *to* 8 ***do***
for $i_2 \leftarrow 1$ *to* 8 ***do***

$$C_j(i_1, i_2) = B_j(i_1, i_2)/Q(i_1, i_2);$$

end
end

   (b) Compute *T* as shown in equation (3.1) after converting the matrix to row or column vectorization, If $T > 0$, then modify all the non-zero AC coefficients and embed the data using equation (3.2). Let the resultant block be C_j.

3. Combine all the C_j blocks into $I = \{C_1,C_2,\ldots.C_l\}$.
4. For all the blocks repeat step 1 to step 3.

$$T = \sum_{j=2}^{64} c_j \qquad (3.1)$$

$$e = \begin{cases} \frac{c}{|c|}\left|\sqrt[0.94]{c} * 0.9\right| & if\ S = 0, \\ \frac{c}{|c|}\left|\left(\sqrt[1.2]{c} * 1.5\right) - 1\right| & if\ S = 1. \end{cases} \qquad (3.2)$$

Where c is the non-zero AC Coefficient, S is the secret bit and e be the m$\hat{I}$ I version of c. Here $|c|$ is round of c.

3.2 Data Extraction Process

Data Extraction is an inverse process of Data Embedding.

Algorithm:

1. Take an watermarked input image (I)
2. Extract C_j from $I \leftarrow \{C_1,C_2,\ldots.C_l\}$.
3. For each $C_j \in I$
   (a) when $T > 0$
      i. Extract the data bits using (3.3).
      ii. Restore the modified coefficients using (3.4).
   Let the resultant block be E_j.
4. Dequantize the elements of E_j as follows:

for $i_1 \leftarrow 1$ *to* 8 ***do***
for $i_2 \leftarrow 1$ *to* 8 ***do***

$$R_j(i_1, i_2) = E_j(i_1, i_2) \times Q(i_1, i_2);$$

end
end

5. Combine all the blocks R_j to get *I* i.e. $I = \{R_1,R_2,\ldots.,R_l\}$
6. For all embedded $R_j \in I$, repeat step 1 to step 5.

$$I_j = \begin{cases} 0 & if\ e\%2 = 0, \\ 1 & otherwise. \end{cases} \qquad (3.3)$$

$$\bar{c} = \begin{cases} \frac{e}{|c|}\left|(e/0.9)^{0.94}\right| \\ \frac{e}{|e|}\left|(e/1.5)^{1.2} - 1\right| \end{cases} \qquad (3.4)$$

Where $\bar{c}$ is the restored version of original c. Here $|e|$ refer to round of *e*.

Note that the data extraction and embedding is the near-reversible.

ISSN: 1992-8645 www.jatit.org E-ISSN: 1817-3195

4. RESULTS AND DISCUSSIONS

We have implemented our proposed scheme using MATLAB. The behavior of the existing function and proposed functions is shown in Figure 4.1. The behavior of the various functions which are nearer to the proposed function is shown in Figure 4.2. We used 512×512 GIF formatted grayscale images of aerial, airplane, baboon, Barb, Boat, couple, Elaine, goldhill, Lena, pentagon, pepper, truck and Zelda. The existing and proposed scheme performance of each quality metric results is shown in the Figures 4.3 to 4.9.

4.1 Hvs Based Visual Quality Metrics

Image Quality Assessment Metric (IQAM) used for evaluation. The objective evaluation is done with help of assessment models is considered are Embedded Capacity, PSNR, PSNR_HVS, PSNR_HVS_M, SSIM, MSSIM, NK and BER.

Embedded Capacity

We define the embedded capacity as the number of bits that can be embedded in to a watermarked image. This is one of the measurement for evaluating the performance of the embedding scheme. In the near reversible scheme we imply that NK ought to be closer to the most extreme esteem 1 and BER ought to be closer to the greatest esteem 0. the lower limits for the NK and BER of a near reversible scheme can't be settled and an application can settle them as wanted.

Peak Signal-To-Noise Ratio (PSNR)

The phrase peak signal-to-noise ratio, often abbreviated PSNR, is an engineering phrase for the ratio between the maximum possible power of a signal and the power of corrupting noise that affects the fidelity of its representation. Because various signals have a very wide dynamic range, PSNR is usually expressed in provisions of the logarithmic decibel scale.

PSNR is most normally utilized as a measure of nature of recreation of lossy pressure codes (e.g., e.g., for image compression). The flag for this situation is the first information, and the noise is the error presented by compression. When looking at compression codes it is utilized as an estimation to human view of recreation quality, along these lines at times one remaking may give off an impression of being nearer to the first than another, despite the fact that it has a lower PSNR (a higher PSNR would regularly show that the reproduction is of higher quality).

One must be amazingly cautious with the scope of legitimacy of this metric; it is just convincingly substantial when it is utilized to analyze comes about because of the same codec (or codec type) and same content. It is most effortlessly characterized through the Mean Squared Error (MSE) which for two m×n monochrome images I and K where one of the images is viewed as an noisy guess of the other is characterized as in equation 4.1

$$MSE = \frac{1}{mn}\sum_{i=0}^{m-1}\sum_{j=0}^{n-1}[I(i,j) - K(i,j)]^2 \qquad (4.1)$$

The PSNR (in db) is defined in equation 4.2 as

$$PSNR = 10log_{10}\left(\frac{MAX_I^2}{MSE}\right) \qquad (4.2)$$

Here, MAX_I is the maximum possible pixel value of the image. When the pixels are represented using 8 bits per sample, this is 255.

For color pictures with three RGB values for every pixel, the meaning of PSNR is the same aside from the MSE is the total over all squared value contrasts separated by picture estimate and by three. On the other hand, for shading pictures the picture is changed over to an alternate shading space and PSNR is accounted for against each channel of that shading space. Common value for the PSNR in lossy picture and video compression are in the between of 30 and 50 dB, where higher is better. Adequate values for remote transmission quality loss are thought to be around 20 dB to 25 dB. At the point when the two pictures are indistinguishable, the MSE will be zero. For this value the PSNR is vague picture.

PSNR_HVS

The Peak signal-to-noise ratio while taking into account the Human Visual System as defined in equation 4.3

$$PSNR\_HVS = 10log_{10}\left(\frac{255^2}{MSE_{HVS}}\right) \qquad (4.3)$$

ISSN: 1992-8645 www.jatit.org E-ISSN: 1817-3195

In this expression, MSE_H is calculated taking into account HVS and defined as in equation 4.4.

$$MSE_H = K\sum_{i=1}^{I-7}\sum_{j=1}^{J-7}\sum_{m=1}^{8}\sum_{n=1}^{8}\left(\left(X[m,n]_{ij} - X[m,n]_{ij}^{e}\right)T_c[m,n]\right)^2 \quad (4.4)$$

Where I, J denote image size, $k = \frac{1}{[(I-7)(J-7)64]}$, X_{ij} are DCT coefficients of 8×8 image block for which the coordinates of left upper corner are equal to i and j, X^e_{ij} are the DCT coefficients of the equivalent block in original image, and T_c is the matrix of correcting factors which is consider from JPEG still picture compression.

The matrix T_c has following properties:

- The proportion among its coefficients is conversely relative to proportion of comparing components in quantization table of JPEG.
- The aggregate adjusting factor of the matrix is $\sum_{m=0}^{8}\sum_{n=0}^{8} T_c[m,n]^2/64$ equivalent to unity. This guarantees if there should arise an occurrence of uniform dissemination of distortions between every single spatial recurrence the estimations of MSE_H corresponds with MSE.

PSNR_HVS_M

PSNR_HVS_M [7] takes into account visual between-coefficient contrast masking of DCT basis functions based on HVS and contrast sensitivity function (CSF).

$$PSNR\_HVS\_M = 10\log_{10}\left(\frac{255^2}{MSE_{HVS\ M}}\right) \quad (4.5)$$

STRUCTURAL SIMILARITY (SSIM) INDEX

Another rationality for image QA in light of the estimation of basic data in a picture, which has since gotten huge perceivability in the exploration group, not with standing across the board appropriation in the picture and video industry. Target techniques for accessing perceptual picture quality generally endeavored to measure the visibiliy of errors (differences) between a distored picture and a reference picture utilizing an assortment of known properties of the human visual system.

The SSIM index implicitly expect that subjective assessment can be isolated into three relating tasks luminance examination, contrast comparison and structure comparison. These comparisions are done locally finished image patches.

Intitially, the luminance of each signal is compared. Assuming discrete signals, this is estimated as the mean intensity (μ) as in the equation 4.6.

$$\mu_x = \frac{1}{N}\sum_{i=1}^{N} x_i \quad (4.6)$$

next, we remove the mean intensity from the signal. The standard deviation is an estimate of the signal contrast using the equation 4.7.

$$\sigma_x = \left(\frac{1}{N-1}\sum_{i=1}^{N}(x_i - \mu_x)^2\right) \quad (4.7)$$

lastly, the signal is normalized (divided) by its own standard deviation, so that the two signals being compared have unit standard deviation. Finally, using the three components are combined to provide an overall similarity measure defined in equation 4.8.

$$S(x,y) = f(l(x,y), c(x,y), s(x,y)) \quad (4.8)$$

The following conditions to satisfy the SSIM to get the result.

Symmetry: S(x,y)=S(y ,x). While evaluating the comparability between two signals, trading the request of information flag ought not influence the outcome

Boundedness: S(x,y)≤1 . Upper bound can serve as an indication of how close two signals are to being perfectly identical.

Unique maximum: S(x,y)=1 iff x=y. SSIM measure should count any variations between input signals.

Therefore this results in below equation 4.9.

Journal of Theoretical and Applied Information Technology
15th February 2018. Vol.96. No 3

ISSN: 1992-8645 www.jatit.org E-ISSN: 1817-3195

$$SSIM(x,y) - \frac{(2\mu_x\mu_y)(2\sigma_{xy})}{(\mu_x^2+\mu_y^2+C_1)(\sigma_x^2+\sigma_y^2+C_2)} \quad (4.9)$$

Where μ_x ,μ_y are mean of X and Y signal and σ_x, σ_y are variance of X and Y signal. Where $C_1 = (K_1 L)^2$ and$K_1 \ll 1$, $C_2 = (K_2 L)^2$ and$K_2 \ll 1$, $C_3 = C_2/2$ and L is the dynamic range of pixel values.

The mean SSIM (MSSIM) index evaluates the overall image quality as defined in equation 4.10

$$MSSIM(X,Y) = \frac{1}{M} SSIM(x_j, y_j) \quad (4.10)$$

Where X and Yare the references and the distorted images, respectively; x_j and y_j are the image contents at the j^{th} local window; and M is the number of local windows of the image.

Normalized Cross Correlation (NK)

In seismology, connection is regularly used to look for comparative signals that are rehashed in a period arrangement this is known as coordinated separating. Since the connection of two high adequacy signals will tend to give huge numbers, one can't decide the closeness of two signals just by looking at the amplitude of their cross relationship. Normalized Cross-Correlation checks the similarity between the reference data and extracted data given in equation 4.11.

$$NK = \frac{\sum_{x,y} N_{x,y} \bar{N}_{x,y}}{\sum_{x,y} (N_{x,y})^2} \quad (4.11)$$

Where N is pixel of the reference image and $\bar{N}$ is pixel of the extracted image. Here NK have two values 0 and 1. NK=0 means N and $\bar{N}$ are completely uncorrelated, NK=1 means N and $\bar{N}$ are highly correlated [8].

BIT ERROR RATE (BER)

Bit error rate also checks the similarity between the reference data and extracted data [13].

$$BER = \frac{INCORRECT}{TOTAL} \quad (4.12)$$

Where INCORRECT= Number of incorrect bits in the extracted data,

TOTAL= Total number of bits in the reference data and BER belongs to 0 and 1.

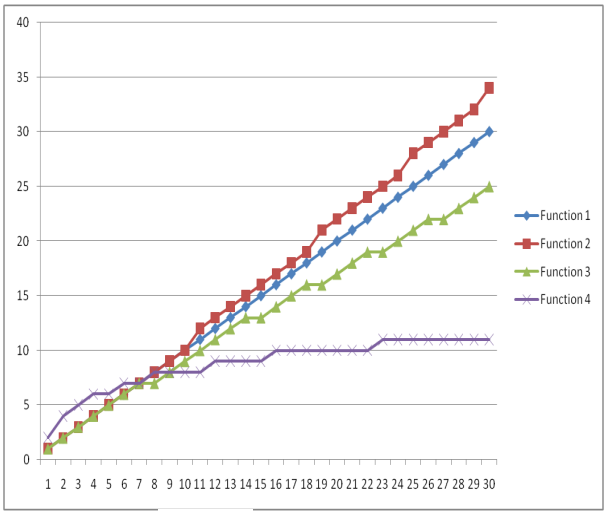

Figure 4.1: Behavior Of Existing Function And Proposed Functions

Where Function 1 is y=AC coefficients of original image,

Function 2 is $y = \left|\sqrt[0.94]{c} * 0.9\right|$,

Function 3 is $y = \left|\left(\sqrt[1.2]{c} * 1.5\right) - 1\right|$,

And Function 4 is $y = \lfloor 2\ log_2(2|c|) \rfloor$.

Where c be the non-zero AC coefficient and y be the modified version of c.

From the above graph, we can observe that the function 4 changes drastically with respect to their original coefficients which cause the distortion or blocking artifacts. From function 2 and function 3 graphs it is observed that the pixel values are nearer to function 1. We considered the functions 2 and 3 are used to embed the data.

Journal of Theoretical and Applied Information Technology
15th February 2018. Vol.96. No 3

ISSN: 1992-8645 www.jatit.org E-ISSN: 1817-3195

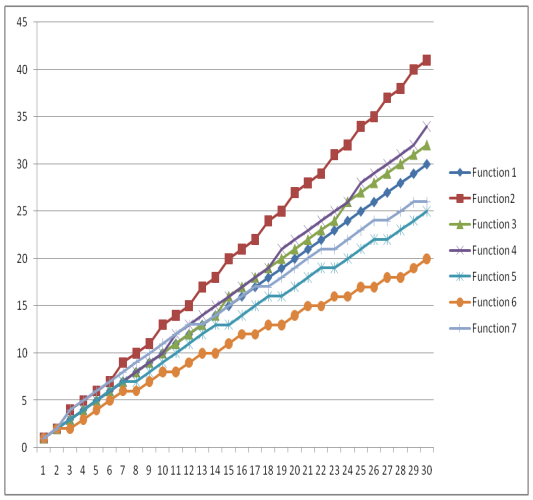

Figure 4.2: Behavior Of Various Functions Nearer To The Proposed Function

Where Function 1 is $y = AC$ coefficients of original image,

Function 2 is $y = \left|\sqrt[0.94]{c} * 1.1\right|$,

Function 3 is $y = \left|\sqrt[0.95]{c} * 0.9\right|$,

Function 4 is $y = \left|\sqrt[0.94]{c} * 0.9\right|$,

Function 5 is $y = \left|\left(\sqrt[1.2]{c} * 1.5\right) - 1\right|$,

Function 6 is $y = \left|\left(\sqrt[1.3]{c} * 1.5\right) - 1\right|$,

and Function 7 is $y = \left|\left(\sqrt[1.3]{c} * 2\right) - 1\right|$

Where c be the non-zero AC coefficient and y be the modified version of c. Here among six functions we can observe two functions nearer to function 1 than other functions are function 4 and function 5. Hence the above two equations are considered in code because they retain maximum values to original values. Here we have chosen function 4 and 5 for hiding the data.

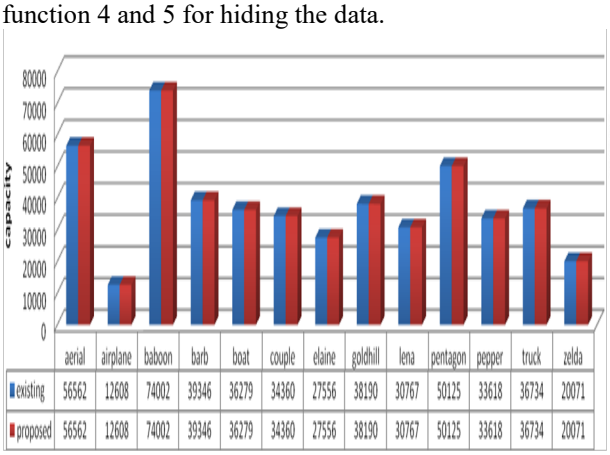

Figure 4.3: Comparison of Capacity

We can observe from the figure 4.3 that existing scheme (in blue color) and proposed scheme (in red color) address same. And for some images there are more number of non-zero AC coefficients, we achieve higher capacity and whenever there is less number of non-zero AC coefficients, we achieve less capacity.

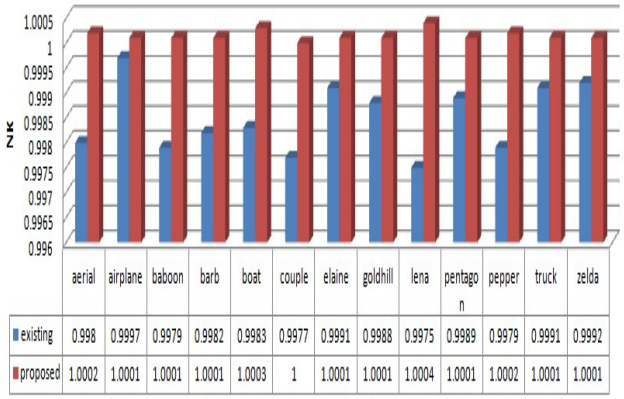

Figure 4.4: Comparison of NK

As the Normalized Cross-Correlation checks the similarity between images means the image before embedding the data and after the where $NK \in [0, 1]$ and more the value near to one the more they are highly correlated, we can achieve them from figure 4.4 that the proposed scheme (in red color) achieve values more nearer to one than the existing scheme (in blue color). Hence, proposed scheme is highly correlated and proposed scheme achieves better NK than the existing scheme.

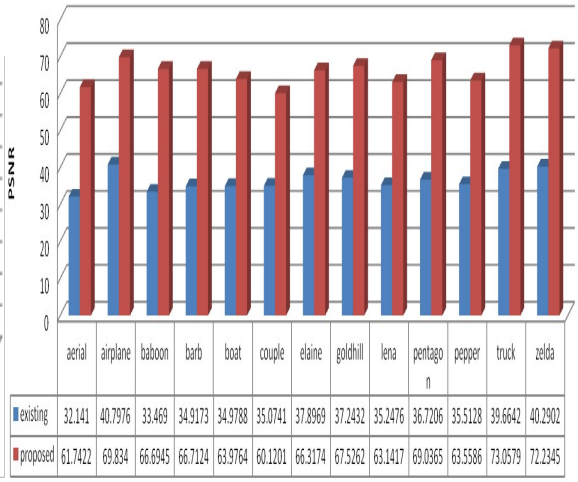

Figure 4.5*: Comparison Of PSNR*

ISSN: 1992-8645 www.jatit.org E-ISSN: 1817-3195

We can observe from figure 4.5 that the proposed scheme (in red color) achieves better results for PSNR than the existing scheme (in blue color).

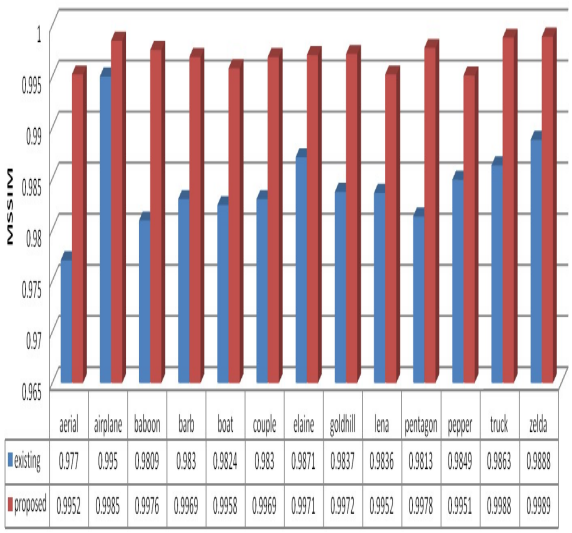

	aerial	airplane	baboon	barb	boat	couple	elaine	goldhill	lena	pentagon	pepper	truck	zelda
existing	0.977	0.995	0.9809	0.983	0.9824	0.983	0.9871	0.9837	0.9836	0.9813	0.9849	0.9863	0.9888
proposed	0.9952	0.9985	0.9976	0.9969	0.9958	0.9969	0.9971	0.9972	0.9952	0.9978	0.9951	0.9988	0.9989

Figure 4.6*: Comparison of (Mean SSIM) MSSIM*

We can observe from figure 4.6 that the proposed scheme (in red color) achieves better results for MSSIM i.e. results are nearer to one (structures in embedded image are more similar to Original image). Therefore, proposed scheme achieves better result for MSSIM than the existing scheme (in blue color).

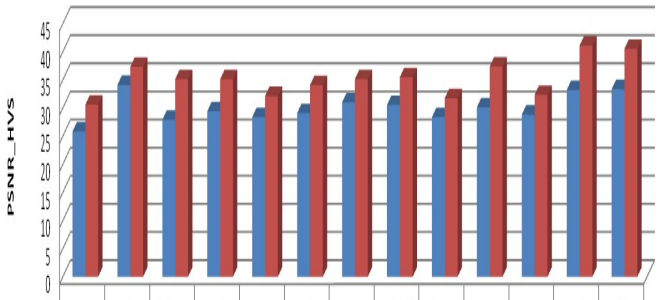

	aerial	airplane	baboon	barb	boat	couple	elaine	goldhill	lena	pentagon	pepper	truck	zelda
existing	25.8168	34.1044	27.9046	29.4258	28.3857	29.1022	30.9839	30.537	28.386	30.1236	28.8172	33.2026	33.3486
proposed	30.5758	37.3014	35.1301	35.1043	32.1248	34.0478	35.1421	35.4885	31.7454	37.3714	32.333	41.0897	40.5373

Figure 4.7*: Comparison of PSNR_HVS*

We can observe from figure 4.7 that the proposed scheme (in red color) achieves better results for all the images than the existing scheme (in blue color) for PSNR_HVS. Therefore, proposed scheme performs better than the existing scheme.

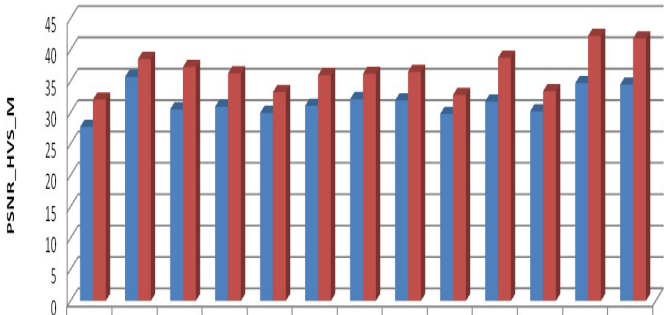

	aerial	airplane	baboon	barb	boat	couple	elaine	goldhill	lena	pentagon	pepper	truck	zelda
existing	27.7434	35.7368	30.5262	30.9697	29.9767	31.102	32.1784	31.9684	29.8235	31.8058	30.2371	34.7113	34.5154
proposed	32.0989	38.5642	37.2993	36.2757	33.3077	35.989	36.2087	36.5304	32.839	38.779	33.4329	42.2659	41.845

Figure 4.8: Comparison of PSNR_HVS_M

We can observe from figure 4.8 that the proposed scheme (in red color) achieves better results for PSNR_HVS_M for all the images than the existing scheme (in blue color). Therefore, proposed scheme performs better than the existing scheme.

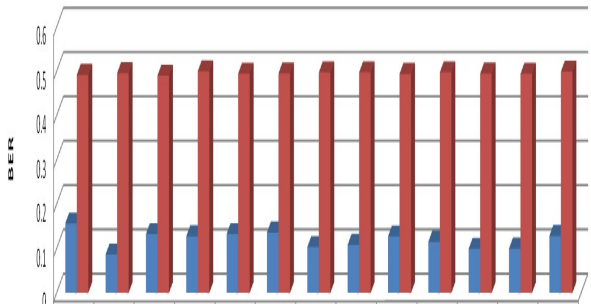

	aerial	airplane	baboon	barb	boat	couple	elaine	goldhill	lena	pentagon	pepper	truck	zelda
existing	0.1568	0.0867	0.1328	0.1277	0.1329	0.1362	0.1034	0.1085	0.1273	0.1153	0.0994	0.1	0.1284
proposed	0.492	0.4959	0.4902	0.5004	0.4948	0.4954	0.4976	0.4979	0.4943	0.4979	0.4951	0.4947	0.4992

Figure 4.9: Comparison of Bit Error Rate

We can observe from figure 4.9 that the existing scheme (in blue color) achieves result for bit error rate is nearer to 0.1 i.e. nearer to zero where as proposed scheme (in red color) achieves values for bit error rate is in range of 0.4 -0.5. Therefore, existing scheme performs better compared to bit error rate of proposed scheme.

We use different images of Barb, Boat, couple, Elaine, Lena, pepper and Zelda GIF format of size

Journal of Theoretical and Applied Information Technology
15th February 2018. Vol.96. No 3

ISSN: 1992-8645 www.jatit.org E-ISSN: 1817-3195

512 × 512 images and their corresponding distorted images can also be observed from all the observations, we can find that the existing scheme distorts the images more where as the proposed scheme achieves better visual quality which will be shown in the Figure 4.10 to. 4.16.

To understaWe formulate tabularly the each image, all quality metrics separately of existing and proposed scheme will be shown in Table 1 to Table 7.

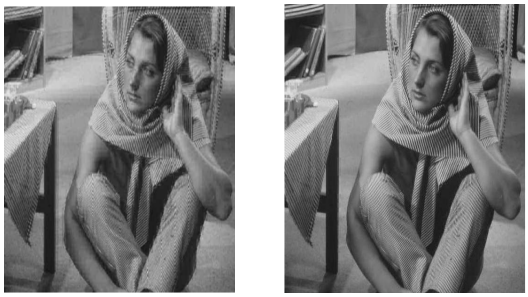

Figure 4.10: View Of The Embedded Barb Image Of Existing And Proposed Scheme

A) Existing Watermark Image B)Proposed Watermark Image

Table 1. Barbe image quality Metrics of Existing and Proposed Scheme

Figure 4.11: Embedded Boat Image Of Existing And Proposed Scheme

A) Existing Watermark Image B)Proposed Watermark Image

Table 2. Boat image quality Metrics of Existing and Proposed Scheme

Metric	Existing	Proposed
Capacity	39346	39346
NK	0.9982	1.0001
PSNR	34.9173	66.7124
MSSIM	0.983	0.9969
PSNR_HVS	29.4258	35.1043
PSNR_HVS_M	30.9697	36.2757
BER	0.1277	0.5004

Metric	Existing	Proposed
Capacity	36279	36279
NK	0.9983	1.0003
PSNR	34.9788	63.9764
MSSIM	0.9824	0.9958
PSNR_HVS	28.3857	32.1248
PSNR_HVS_M	29.9767	33.3077
BER	0.1329	0.4948

Figure 4.12: Embedded Couple Image Of Existing And Proposed Scheme

A) Existing Watermark Image B)Proposed Watermark Image

Table 3. Couple image quality Metrics of Existing and Proposed Scheme

Metric	Existing	Proposed
Capacity	34360	34360
NK	0.9977	1
PSNR	35.0741	60.1201
MSSIM	0.983	0.9969
PSNR_HVS	29.1022	34.0478
PSNR_HVS_M	31.102	35.989
BER	0.1362	0.4954

ISSN: 1992-8645 www.jatit.org E-ISSN: 1817-3195

Figure 4.13: Embedded Elaine Image Of Existing And Proposed Scheme
A) Existing Watermark Image B)Proposed Watermark

Table 4. Elaine Image Quality Metrics Of Existing And Proposed Scheme

Metric	Existing	Proposed
Capacity	27556	27556
NK	0.9991	1.0001
PSNR	37.8969	66.3174
MSSIM	0.9871	0.9971
PSNR_HVS	30.9839	35.1421
PSNR_HVS_M	32.1784	36.2087
BER	0.1034	0.4976

Figure 4.14: Embedded Lena Image Of Existing And Proposed Scheme

A) Existing Watermark Image B)Proposed Watermark Image

Table 5. Lena Image Quality Metrics Of Existing And Proposed Scheme

Metric	Existing	Proposed
Capacity	30767	30767
NK	0.9975	1.0004
PSNR	35.2476	63.1417
MSSIM	0.9836	0.9952
PSNR_HVS	28.386	31.7454
PSNR_HVS_M	29.8235	32.839
BER	0.1273	0.4943

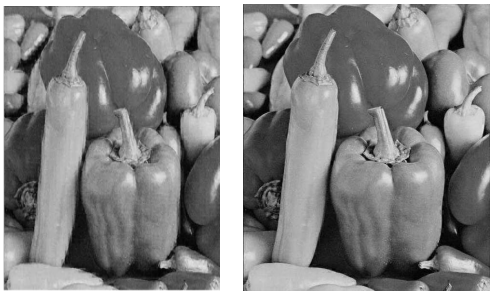

Figure 4.15: Embedded Pepper image of existing and proposed scheme
a) Existing watermark image b)Proposed watermark image

Table 6. Pepper image quality Metrics of Existing and Proposed Scheme

Metric	Existing	Proposed
Capacity	33618	33618
NK	0.9979	1.0002
PSNR	35.5128	63.5586
MSSIM	0.9849	0.9951
PSNR_HVS	28.8172	32.333
PSNR_HVS_M	30.2371	33.4329
BER	0.0994	0.4951

Figure 4.16: Embedded Zelda Image Of Existing And Proposed Scheme

A) Existing Watermark Image B)Proposed Watermark Image

ISSN: 1992-8645 www.jatit.org E-ISSN: 1817-3195

Table 7. Zelda Image Quality Metrics Of Existing And Proposed Scheme

Metric	Existing	Proposed
Capacity	20071	20071
NK	0.9992	0.4992
PSNR	40.2902	72.2345
MSSIM	0.9888	0.9989
PSNR_HVS	33.3486	40.5373
PSNR_HVS_M	34.5154	41.845
BER	0.1284	0.4992

The results what we observed in literature survery specifically considering the qualty of multimedia content by using metric like PSNR. In this paper we considering to access the overall quality of multimedia content by using the Human Visual System based metrics like PSNR_HVS, PSNR_HVS_M, MSSIM.

5. CONCLUSION

With the proposed of the new category near-reversible data embedding, there is a need for more sophisticated scheme. There are many applications in remote sensing which can be addressed by near reversible schemes. The existing scheme degrades the visual quality and creates many blocking artifacts due to use of log function which transforms the coefficients with larger difference. The proposed scheme achieves higher visual quality as it minimizes the difference between original non-zero AC coefficients to the embedded coefficients. This scheme can be applied to video also. HVS based visual quality metrics are used to access the visual quality of the degraded content. However there is a little drawback when concerned bit error rate.

REFERENCES:

[1] Sagar Gujjunoori, B. B. Amberker, "A DCT Based Near Reversible Data Embedding Scheme for MPEG-4 Video," Proceedings of the Fourth International Conference on Signal and Image Processing 2012 (ICSIP 2012), pp 69-79, 2013.

[2] Fridrich J, Du R, "Lossless authentication of MPEG-2 video," In: ICIP'02, pp 893–896, 2002.

[3] Sagar G, Amberker BB, "A DCT based reversible data hiding scheme for mpeg-4 video," In: Proceedings of international conference on signal, Image and Video Processing (ICSIVP) 2012, IIT Patna, pp 254–259, Jan 2012.

[4] Zeng X, Chen Z, Zhang X, "Issues and solution on distortion drift in reversible video data hiding," Multimedia Tools Appl 52(2–3):465–484, 2011.

[5] Barni M, Bartolini F, Cappellini V, Magli E, Olmo G, " Near-lossless digital watermarking for copyright protection of remote sensing images," IGARSS '02., vol 3, pp 1447–1449, 2002.

[6] K. Egiazarian, J. Astola, N. Ponomarenko, V. Lukin, F. Battisti, M. Carli, " New full-reference quality metrics based on HVS," CD-ROM Proceedings of the Second International Workshop on Video Processing and Quality Metrics, Scottsdale, USA, 4 p, 2006.

[7] N. Ponomarenko, F. Silvestri, K.Egiazarian, M. Carli, V. Lukin, "On Between-Coefficient Contrast Masking of DCT Basis Functions," CD-ROM proceedings of Third International Workshop on Video Processing and Quality Metrics for Consumer Electronics VPQM-07, 4p, January 2007.

[8] Zhou Wang, Alan Conrad Bovik, Hamid Rahim Sheikh, Eero P. Simoncelli, "Image Quality Assessment: From Error Visibility to Structural Similarity," vol. 13, NO. 4, APRIL 2004.

[9] Hsu C-T, Wu J-L, "Hidden digital watermarks in images," IEEE Trans Image Process 8(1):58–68, 1999.

[10] Ahmed F, Moskowitz, "A semi-reversible watermark for medical image authentication," In:1st Transdisciplinary conference on distributed diagnosis and home healthcare. D2H2, pp 59–62, 2006.

[11] Tang Y-L, Huang H-T, "Robust near-reversible data embedding using histogram projection," In: In IIH-MSP 2007, vol 02, pp 453–456, 2007.

[12] Zhang B, Xin Y, Niu X-X, Yuan K-G, Jiang H-B, "A near reversible image watermarking algorithm," In: International conference on machine learning and cybernetics (ICMLC), vol 6, pp 2824–2828, july 2010.

[13] G. Wallace, "The JPEG still Picture Compression Standard," Comm. of the AC, vol. 34, No. 4, 1991.

[14] T. Movshon and L. Kiorpes, "Analysis of the development of spatial sensitivity in monkey and human infants," JOSA A. vol5, 1998.

[15] P.G. J. Barten, "Contrast Sensitivity of the Human Eye and Its Effects on Image Quality," SPIE, Bellingham, WA, 1999.

ISSN: 1992-8645 www.jatit.org E-ISSN: 1817-3195

[16] S. Daly, "The Visible Differences Predictor: An algorithm for the assessment of image fidelity," Ch. 13 in Digital Images and Human Vision, A.B. Watson Ed., MIT Press, Cambridge, MA, 1993.

[17] M. P. Eckert and A. P. Bradley, "Perceptual quality metrics applied to still image compression," Signal Processing, vol. 70, pp. 177–200, Nov. 1998.

[18] E. P. Simoncelli," Statistical models for images: compression, restoration and synthesis," in Proc 31st Asilomar Conf. Signals, Systems and Computers, Pacific Grove, CA, pp. 673–678, Nov. 1997.

[19] A. B. Watson, "Visual detection of spatial contrast patterns: evaluation of five simple models," Opt. Exp., vol. 6, pp. 12–33, Jan. 2000.

[20] F. T. Wedaj, S. Kim, H. J. Kim and F. Huang "Improved reversible data hiding in JPEG images based on new coefficient selection strategy" EURASIP Journal on Image and Video Processing20172017:63 https://doi.org/10.1186/s13640-017-0206-1.

[21] M Fujiyoshi and Hitoshi Kiya "Histogram-Based Near-Lossless Data Hiding and Its Application to Image Compression" Advances in Multimedia Information Processing—PCM2015pp225-235.